Electronic Supplementary Material (ESI) for Chemical Communications
This journal is © The Royal Society of Chemistry 2013

A robust amino-functionalized Titanium (IV) based MOF for an improved separation of acid gases

Sébastien Vaesen,[a] *Vincent Guillerm,*[b] *Qingyuan Yang,*[c,g] *Andrew Wiersum,*[d] *Bartosz Marszalek,*[e] *Barbara Gil,*[e] *Alexandre Vimont,*[f] *Marco Daturi,*[f] *Thomas Devic,*[b] *Philip L. Llewellyn,*[d] *Christian Serre*[b]**, *Guillaume Maurin*[c]** *and Guy De Weireld*[a]**

[a] Service de Thermodynamique, Faculté Polytechnique, Université de Mons, 20 Place du Parc, Mons, 7000 (Belgium).
E-mail: guy.deweireld@umons.ac.be
[b] Institut Lavoisier, UMR CNRS 8180–Université de Versailles St Quentin en Yvelines,
45 avenue des Etats-Unis, Versailles, 78035 (France).
E-mail: serre@chimie.uvsq.fr
[c] Institut Charles Gerhardt Montpellier, UMR CNRS 5253, UM2, ENSCM, UM1, Place E. Bataillon, Montpellier cedex 05, 34095 (France).
E-mail: gmaurin@univ-montp2.fr
[d] MADIREL, UMR CNRS 7246 – Aix-Marseille Université, Centre de Saint-Jérôme, Marseille cedex 20, 13397 (France).
[e] Department of Chemistry, Jagiellonian University in Krakow,Ingardena 3, Krakow 30-060 (Poland).
[f] Laboratoire Catalyse et Spectrochimie, ENSICAEN, Université de Caen Basse Normandie, CNRS, 6 Boulevard du Maréchal Juin, Caen, 14050 (France).
[g] State Key Laboratory of Organic-Inorganic Composites, Beijing University of Chemical Technology, Beijing 100029 (China)

Supporting Information

1. Synthesis and characterization

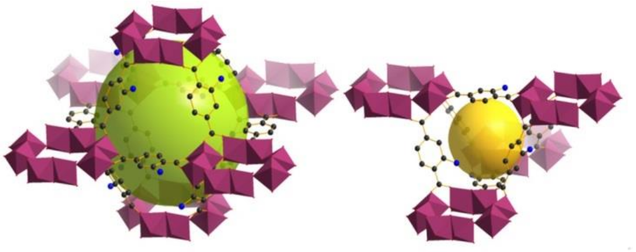

Figure S0. Schematic view of the cages of MIL-125(Ti)-NH_2. Metal polyhedra, carbon, nitrogen and oxygen atoms are in violet, black, blue and red, respectively. Hydrogen atoms have been omitted for clarity.

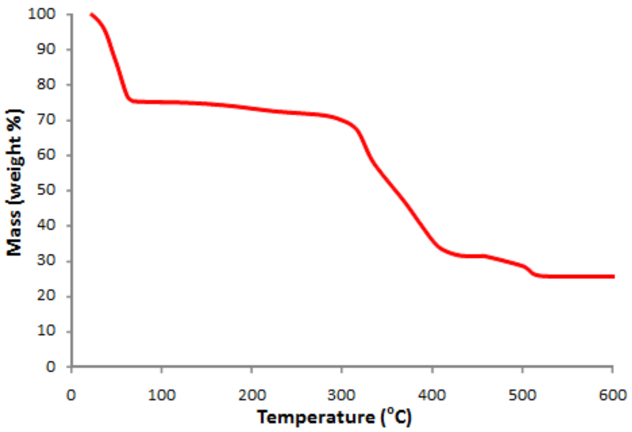

Figure S1. Thermal gravimetric analysis

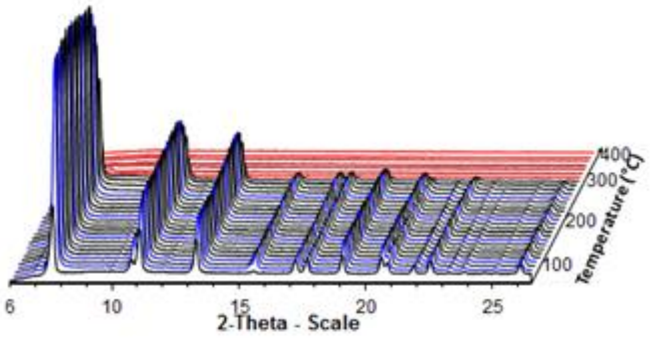

Figure S2. X-Ray thermodiffractometry of MIL-125(Ti)-NH_2 under air atmosphere (λ_{Co}~1.7906Å)

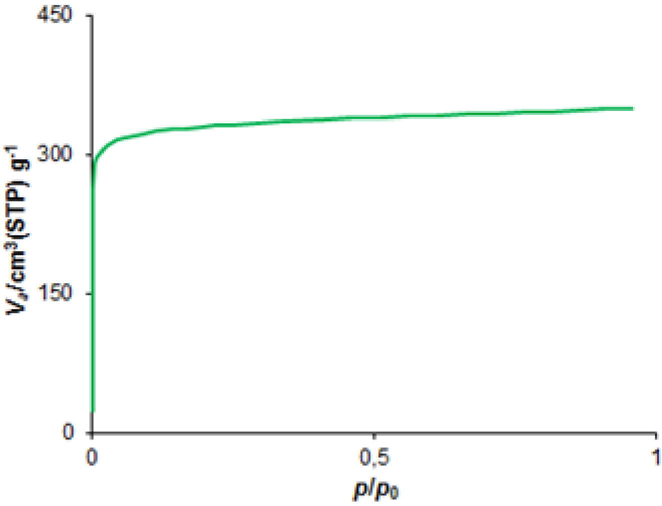

Figure S3. Nitrogen adsorption of MIL-125(Ti)-NH_2 at 77K (P_0=1 bar).

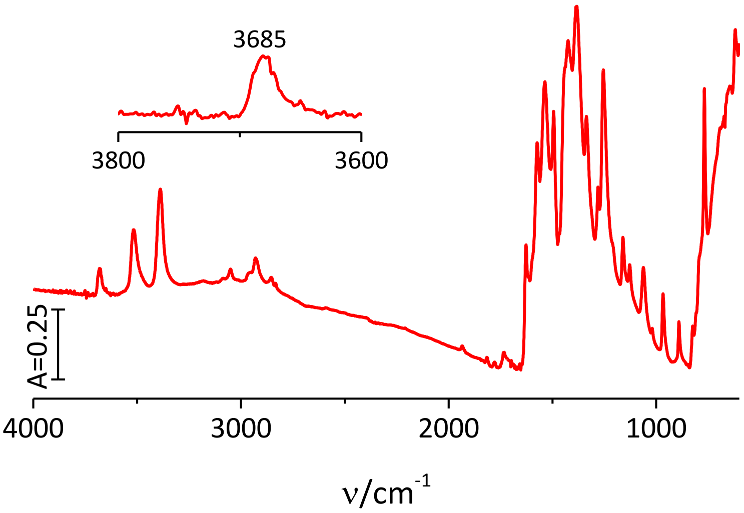

Figure S4. Room temperature IR spectroscopy. Spectrum of MIL-125(Ti)-NH_2 activated at 473K. Insert: the ν(OH) region showing the presence of μ_2-OH groups.

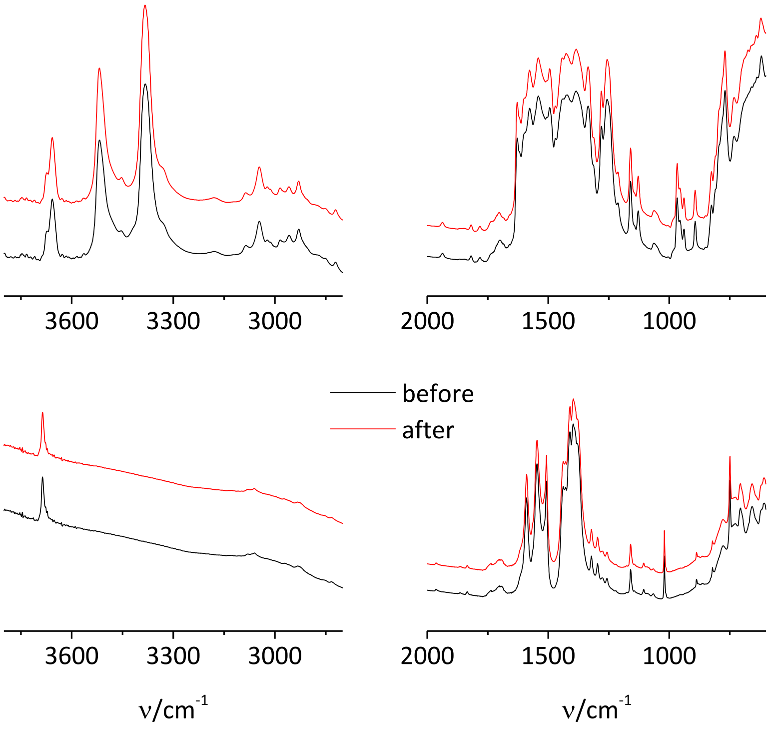

Figure S5. IR spectra of MIL-125(Ti)-NH_2 (top) and MIL-125(Ti) (bottom) before and after exposure to water vapor at 373 K. Spectra at RT, samples before experiment outgassed at 473 K.

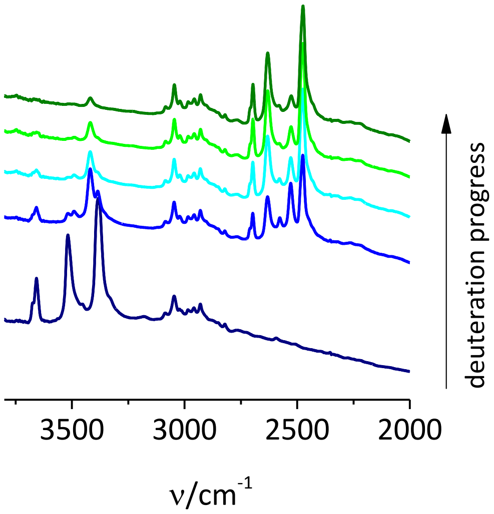

Figure S6. IR spectra of MIL-125(Ti)-NH_2, outgassed at 473 K for 2 hours, after subsequent steps of H/D exchange at 323 K. Before each spectrum saturated D_2O vapor was put in contact with the sample for 1 minute and then evacuated. Some steps were omitted for better clarity of the figure.

2. Single component adsorption measurement

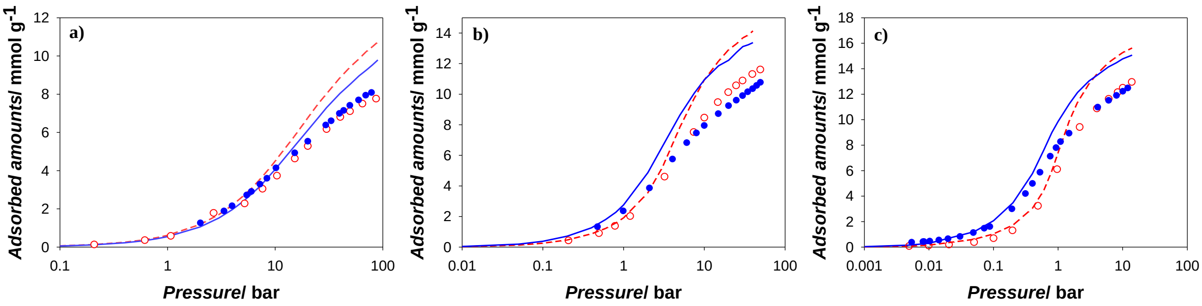

Figure S7. Comparative study of the single component adsorption measurements at 303 K: (a) CH_4; (b) CO_2; (c) H_2S on the parent MIL-125(Ti) (red: dotted lines and empty circle) and its amino derivative (blue: full lines and circles); lines stand for GCMC simulations and points for experimental values.

Table S1. Experimental Henry coefficients and both GCMC simulated and experimental enthalpies at 303 K. Simulated enthalpies are calculated at zero coverage. Experimental enthalpies are measured at an adsorbed loading corresponding to a 0.1 bar equilibrium pressure.

Adsorbent	Compound	*Henry constants [mmol g^{-1} bar^{-1}]*	*Experimental enthalpies [kJ mol^{-1}]*	*Simulated enthalpies [kJ mol^{-1}]*
MIL-125(Ti)	CH_4	0.622	17.4	14.0
	CO_2	1.778	25.8	26.5
	H_2S	6.853	- [1]	31.9
MIL-125(Ti)-NH$_2$	CH_4	0.7159	18.8	14.2
	CO_2	2.846	29.8	28.5
	H_2S	21.27	- [1]	32.7

[1] Enthalpy measurement not possible with the used apparatus (Tian-Clavet microcalorimetry).

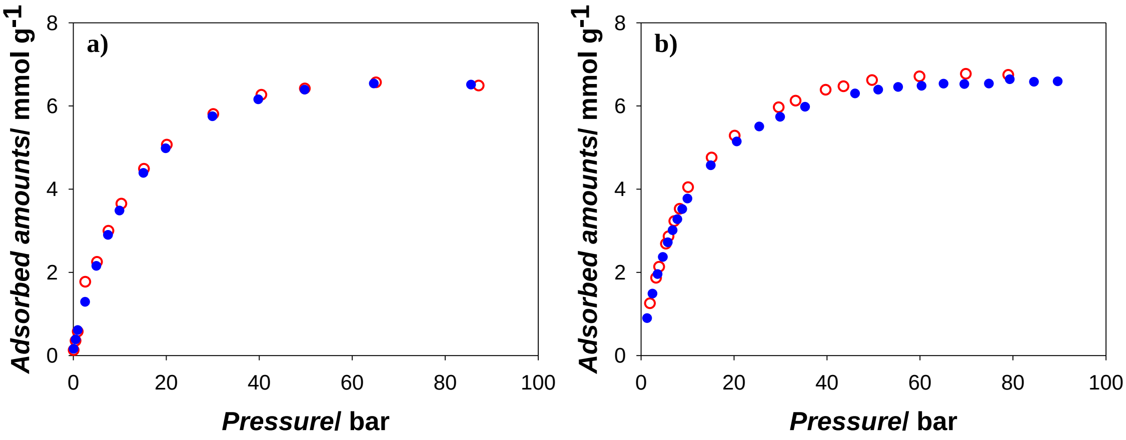

Figure S8. CH_4 excess isotherms (at 303 K) before (red empty circle) and after H_2S adsorption (blue full circles); (a) MIL-125(Ti); (b) MIL-125(Ti)-NH_2

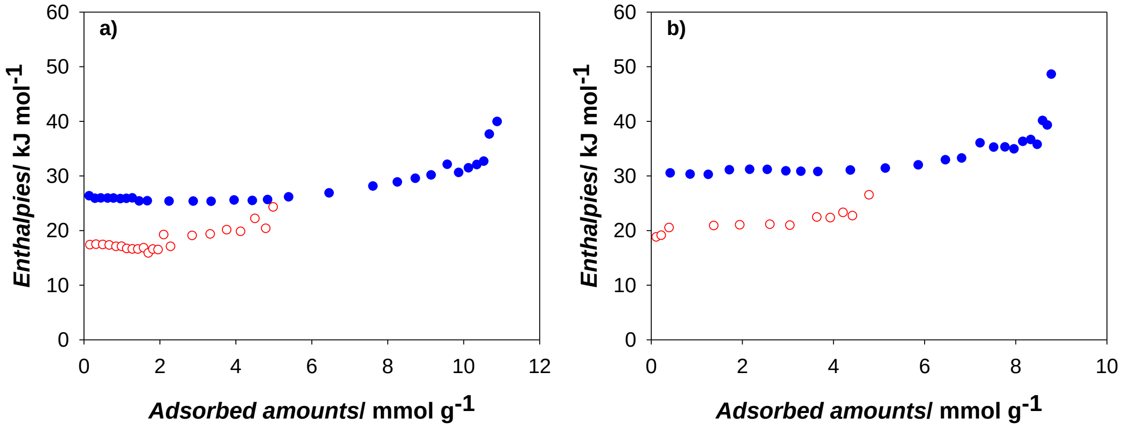

Figure S9. Adsorption enthalpies for methane (open red symbol) and carbon dioxide (close blue symbol) on MIL-125(Ti) (a) and MIL-125(Ti)-NH_2(b)

3. GCMC simulation

3.1. Computational Assisted Structure Determination

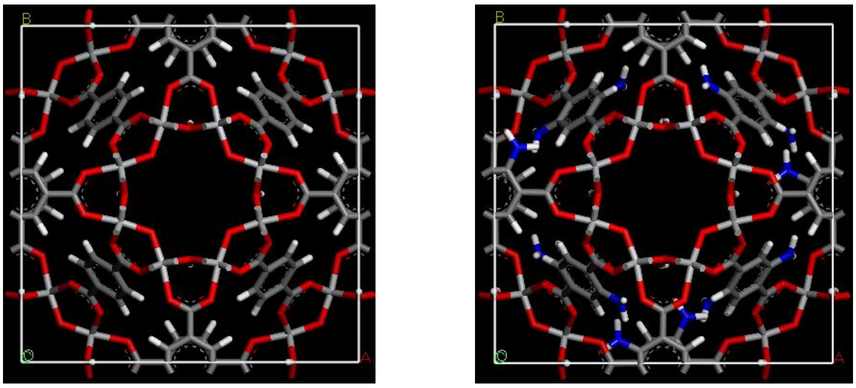

(a) MIL-125(Ti)

(h) MIL-125(Ti)-NH_2

Figure S10. Illustration of the crystal structures of MIL-125(Ti) and MIL-125(Ti)-NH_2 determined by density functional theory (DFT) geometry optimization based on the experimental unit cell parameters extracted from X-ray diffraction measurements.

Table S2. Structural features of the optimized MIL-125(Ti) and MIL-125(Ti)-NH_2

Materials	**Lattice sizes (Å)**[a]	**V_{pore}**[b] **($cm^3.g^{-1}$)**	**S_{acc}**[b] **($m^2.g^{-1}$)**	**ρ_{cyrst}**[c] **($g\ cm^{-3}$)**	**V_{pore}**[c] **($cm^3.g^{-1}$)**	**S_{acc} ($m^2.g^{-1}$)**[b]
MIL-125(Ti)	a = 18.6540 c = 18.1440	0.469	1179	0.825	0.794	2060
MIL-125(Ti)-NH_2	a = 18.6730 c = 18.1380	0.540	1244	0.871	0.722	1730

[a] Obtained from XRD data.

[b] Calculated from experimental N_2 sorption isotherms at 77K.

[c] Simulated values.

The initial atomic coordinates of MIL-125(Ti) was taken directly from the refined structure obtained by X-ray powder diffraction (XRPD) in our previous work.[1] The crystallographic cell parameters for this structure is reminded in Table S3. Since the positions of the H atoms cannot be detected by such experimental techniques, these atoms were added to the terephthalate linkers as well as to the μ_2-O positions according to the chemical composition determined experimentally.[1] The so-obtained structural model was then refined by a periodic density functional theory (DFT) geometry optimization procedure, using the Dmol^3 module implemented in the Materials Studio software.[2] The PW91 GGA functional combined with the double numerical basis set containing polarization function on hydrogen atoms (DNP) were employed in this calculation.

Based on the parent structure of MIL-125(Ti), the starting configuration for its amine-modified form structure was built by (i) substituting the H atoms on the phenyl rings with the $–NH_2$ functional groups, (ii) imposing the unit cell parameters determined from the XRPD refinement (see Tables S2). Further, several initial models were generated by grafting the functional groups onto all the possible positions on the terephthalate linkers. These models were converted into P1 symmetry and then optimized by maintaining the cell parameters fixed. These geometry optimizations were conducted using the Forcite module implemented in Materials Studio software, based on the Universal force field (UFF)[3] and the charges calculated from the Electronegativity Equalization method. The most plausible position for the amino- groups was identified by selecting the optimized structure with the lowest energy. Finally, periodic DFT geometry optimization procedure described above was further employed to refine this selected confguration. The optimized structures for MIL-125(Ti) and MIL-125(Ti)-NH_2 are schematically shown in Figure S10.

3.2. Pore Volume and Accessible Surface Area Calculations

The pore volumes (V_{pore}) of both MIL-125(Ti)s reported in Table S2 were obtained according to the thermodynamic method proposed by Myers and Monson.[4] In these calculations, the

UFF[3] force field was used to describe the Lennard-Jones (LJ) interactions of each framework atom while the LJ parameters for Helium (ε/k_B = 10.9 K, σ = 2.64 Å) were taken from the work of Talu and Myers.[5] The accessible surface area (S_{acc}) given in Table S2 for each MIL-125(Ti) is purely based on its geometric topology and was calculated from a simple Monte Carlo integration technique where the center of mass of the probe molecule with hard sphere is "rolled" over the framework surface.[6] In this method, a nitrogen-sized (3.6 Å) probe molecule is randomly inserted around each framework atom of the adsorbent and the fraction of the probe molecules without overlapping with the other framework atoms is then used. The LJ size parameters of the framework atoms were the same as those used for the calculations of the pore volume.

3.3. Pore Size Distribution Calculations

The geometric methodology reported by Gelb and Gubbins[7] was used to calculate the pore size distributions (PSD) of the MIL-125(Ti) and MIL-125(Ti)-NH_2 structures. In these calculations, the van der Waals parameters of the framework atoms were adopted from UFF. This method has been widely used to characterize the pore size of various nanoporous adsorbents.[6] The corresponding results for these two MOFs are shown in Figure S11.

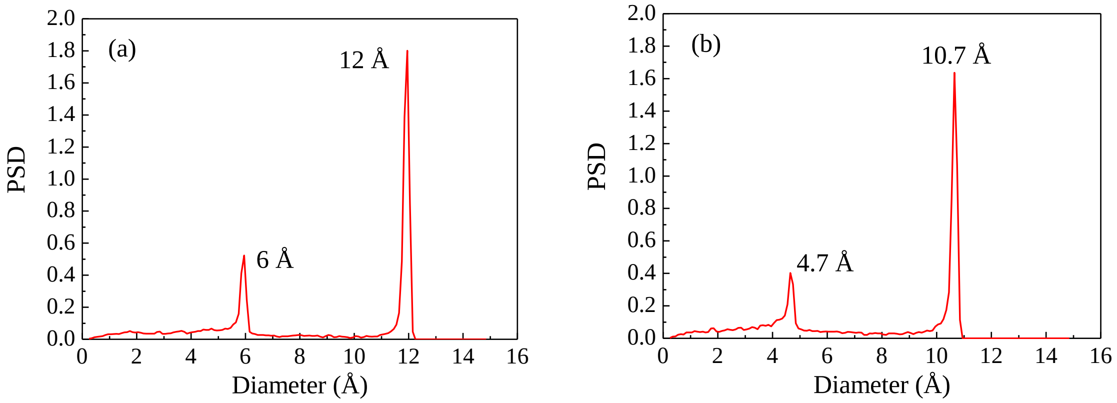

Figure S11. Comparsion of the pore size distributions for MIL-125(Ti) and MIL-125(Ti)-NH_2.

3.4. Atomic Partial Charge Calculations

As we previously reported for other MOFs,[8-9] the partial charges for each framework atom of MIL-125(Ti) and MIL-125(Ti)-NH_2 were extracted from periodic DFT calculations using the Mulliken charge partitioning method implemented in Dmol^3 with the same functional and basis set as those described above for the structural optimizations (Figure S12 and S13; Table S3 and S4).

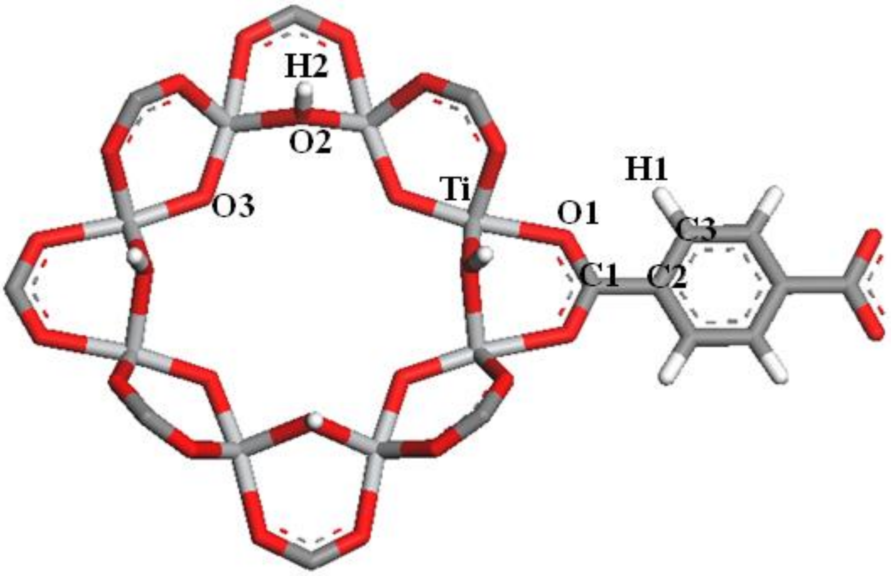

Figure S12. Labels of the atoms for the inorganic and organic parts of MIL-125(Ti) as employed in Table S3.

Table S3. Atomic partial charges for the MIL-125(Ti) structure derived on DFT/PW91 Level.

Atomic types	**Ti**	**O1**	**O2**	**O3**	**C1**	**C2**	**C3**	**H1**	**H2**
Charge (e)	1.387	–0.551	–0.651	–0.722	0.614	–0.086	–0.072	0.138	0.288

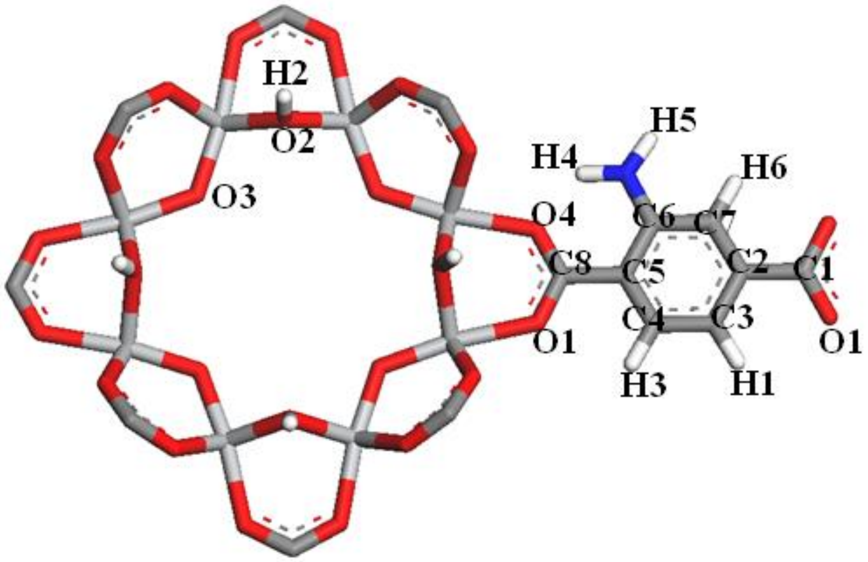

Figure S13. Labels of the atoms for the inorganic and organic parts of MIL-125(Ti)-NH_2 as employed in Table S3.

Table S4. Atomic partial charges for the MIL-125(Ti)-NH_2 structure derived on DFT/PW91 Level.

Atomic types	**Ti**	**O1**	**O2**	**O3**	**O4**	**C1**	**C2**	**C3**	**C4**	**C5**
Charge (e)	1.384	–0.554	–0.666	–0.726	–0.616	0.609	–0.074	–0.098	–0.074	–0.130
Atomic types	**C6**	**C7**	**C8**	**H1**	**H2**	**H3**	**H4**	**H5**	**H6**	**N**
Charge (e)	0.162	–0.124	0.629	0.129	0.305	0.138	0.489	0.440	0.139	–0.837

3.5. Interatomic Potentials

In this study, a single Lennard-Jones (LJ) interaction site model was used to depict a CH_4 molecule with potential parameters taken from the TraPPE forcefield.[10] CO_2 molecule was represented by the conventional rigid linear triatomic model with three charged LJ interaction sites (C–O bond length of 1.149 Ǻ) centred on each atom as developed by Harris and Yung.[11] Finally, H_2S was treated by the three-site model reported by Kamath *et al.*,[12] where only S atom is a LJ interaction site while partial charges are centered on each atom. The H–S bond length is 1.34 Ǻ and the H-S-H angle is 92.5°. All the corresponding atomic partial charges and interatomic potential parameters are given in Table S5, which have been successfully used to reproduce the experimental vapor-liquid phase equilibrium data of each gas.[10-12]

The interactions between the adsorbates and both MIL-125(Ti)s were described by a combination of site-site LJ and Coulombic potentials, except for CH_4 where only a site-site LJ potential was considered. The LJ potential parameters for the framework atoms of MIL-125(Ti)s were taken from Universal Force field (UFF),[3] as given in Table S6. Following the treatment adopted in other well-known forcefields,[13-14] we considered that the hydrogen atoms of the hydroxyl and amino groups interact with the adsorbate molecules only through the Coulombic potential. All the LJ cross interaction parameters including adsorbate/adsorbate and adsorbate/MOF were determined by the Lorentz-Berthelot mixing rule.

Table S5. Potential parameters and partial charges for the adsorbates

Atomic type	σ **(Å)**	ε/k_B **(K)**	q **(e)**
CH_4	3.730	148.000	0.0000
CO_2_C	2.757	28.129	0.6512
CO_2_O	3.033	80.507	–0.3256
H_2S_S	3.710	278.000	–0.2520
H_2S_H			0.1260

Table S6. LJ potential parameters for the atoms of the MOFs studied in this work.

Elements	**UFF**	
	σ **(Å)**	ε/k_B **(K)**
Ti	2.829	8.555
C	3.431	52.841
O	3.118	30.195
H	2.571	22.143
N	3.261	34.724

3.6. Details of the Molecular Simulations

Grand canonical Monte Carlo (GCMC) simulations were performed to investigate the adsorption of the single gases CO_2, CH_4 and H_2S as well as their mixtures in MOFs, using our newly developed simulation code CADSS (Complex Adsorption and Diffusion Simulation Suite). For the simulations of pure components, molecules involve four types of trials: attempts (i) to displace a molecule (translation or rotation), (ii) to regrow a molecule at a random position, (iii) to create a new molecule, and (iv) to delete an existing molecule. For the simulations of mixture, attempt to exchange molecular identity was introduced as an additional type of trial to speed up the equilibrium and reduce the statistical errors. Details on the method can be found elsewhere.[15] For the calculation of the adsorption enthalpies (ΔH) of each gas at the limit of zero-coverage, configurational-bias Monte Carlo simulations in the canonical (NVT) ensemble were further performed using the revised Widom's test particle method.[16]

3.7. Simulated distribution of the adsorbate molecules within the porosity

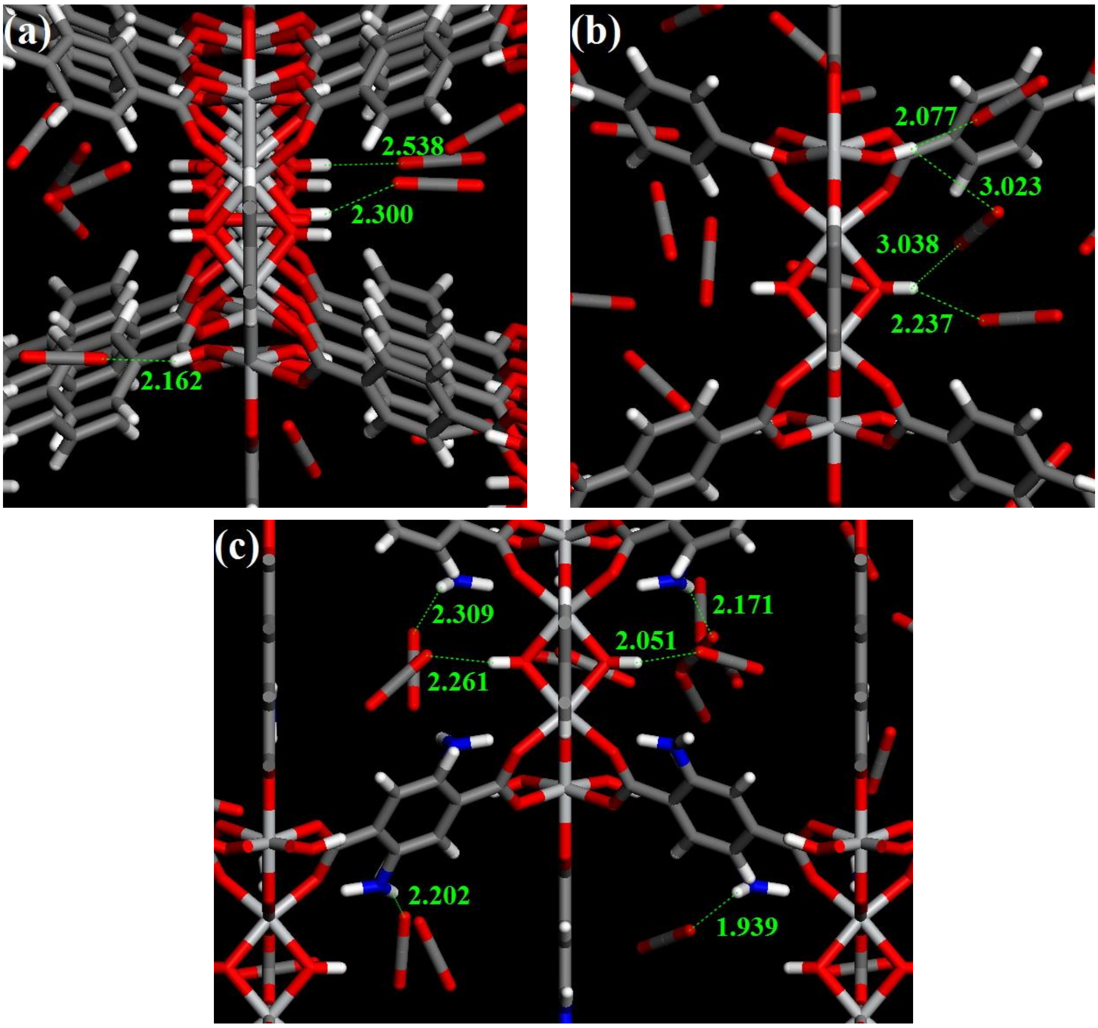

Figure S14. Snapshots extracted from the GCMC simulations at 1.0 bar and 303 K, emphasizing the interactions between the CO_2 molecules and (a) the μ_2-OH groups in MIL-125(Ti) and (c) the μ_2-OH groups and the NH_2 grafted functions in MIL-125(Ti)-NH_2. (b) corresponds to a snapshot extracted from the GCMC simulations at 5 bar and 303K. The distances are reported in Å. (Ti, light grey; O, red; C, gray; H, white and N, blue).

In contrast to snapshots for H_2S and CO_2, the following snapshots evidence that the CH_4 molecules do not give any specific interactions with the pore wall of both MIL-125(Ti) and MIL-125(Ti)-NH_2 which supports that the adsorption enthalpy remains almost unchanged when the solid is grafted with the amino function.

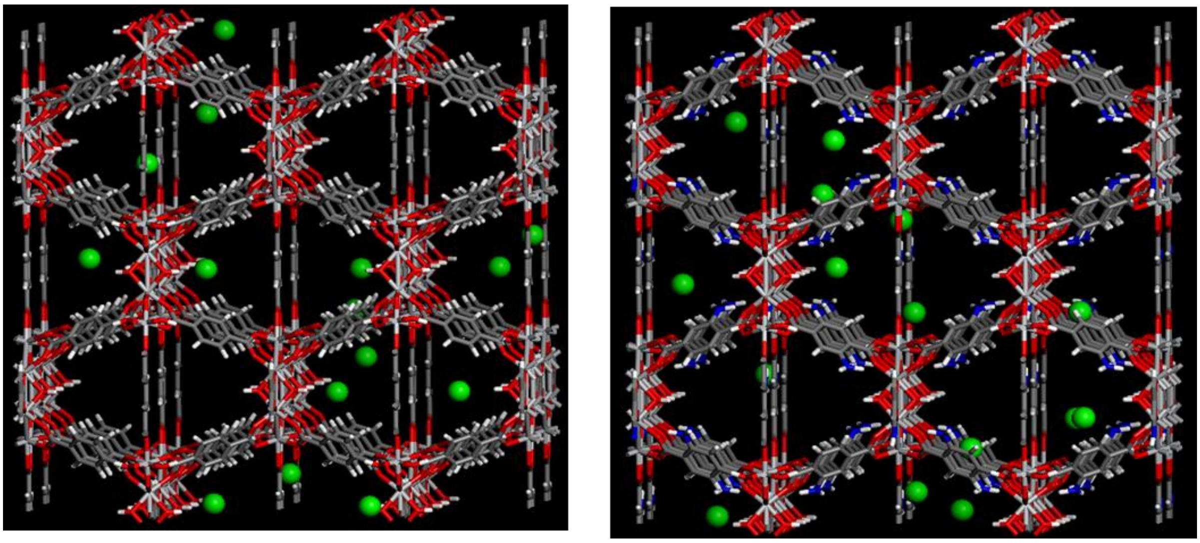

Figure S15. Most preferential arrangement of CH_4 within the porosity of MIL-125(Ti) (left) and MIL-125(Ti)-NH_2 (right) issued from our GCMC simulations realized at 303 K for a pressure of 1 bar.

3.8. Radial Distribution Functions

3.8.1. CO_2 in MIL-125(Ti) and in MIL-125(Ti)-NH_2

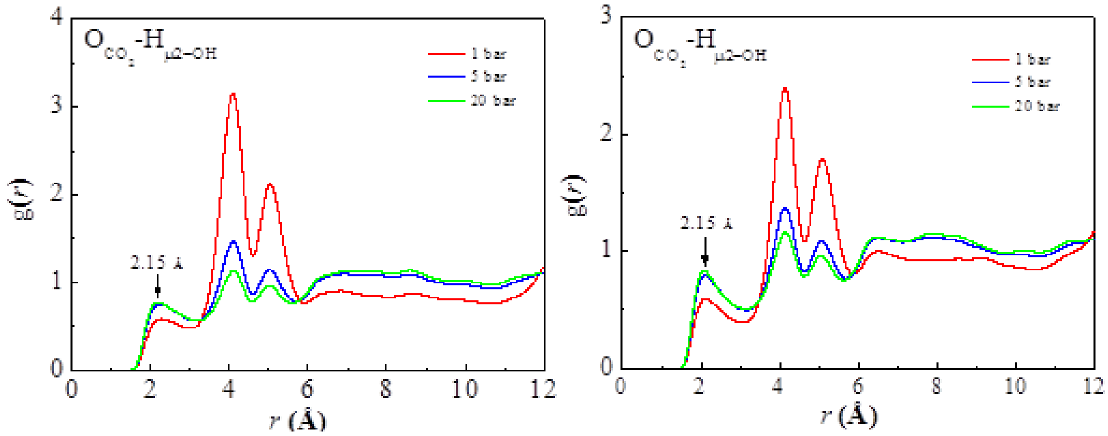

Figure S16. Radial distribution functions for the pair $O(CO_2)$-$H(\mu_2$-$OH)$ in MIL-125(Ti) (left) and MIL-125(Ti)-NH_2 (right) at 303 K at 3 different pressures.

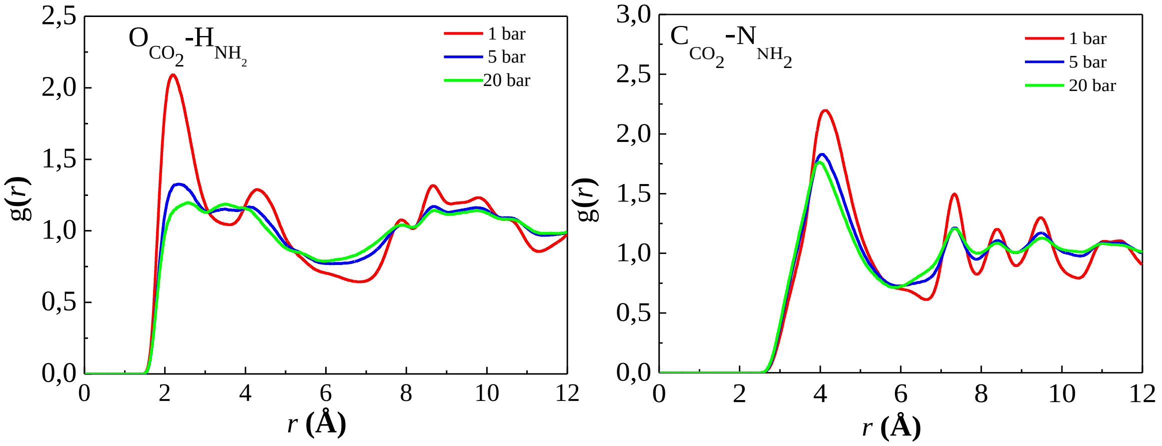

Figure S17. Radial distribution functions for the pairs O(CO_2)-H(NH_2) and C(CO_2)-N(NH_2) in MIL-125(Ti)-NH_2 (left) at 303 K at 3 different pressures.

3.8.2. H_2S in MIL-125(Ti) and in MIL-125(Ti)-NH_2

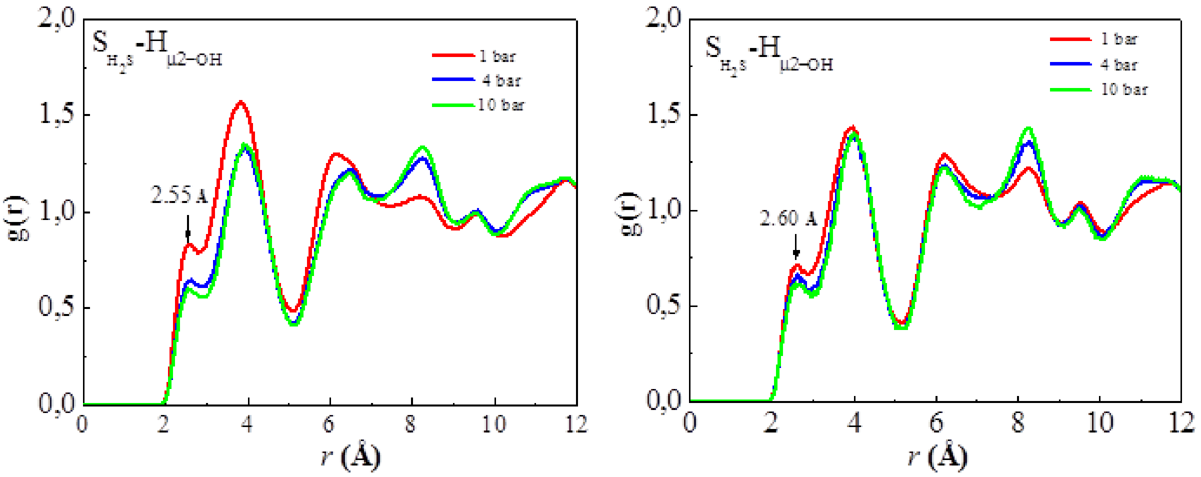

Figure S18. Radial distribution functions for the pair S(H_2S)-H(μ_2-OH) in MIL-125(Ti) (left) and MIL-125(Ti)-NH_2 (right) at 303 K at 3 different pressures.

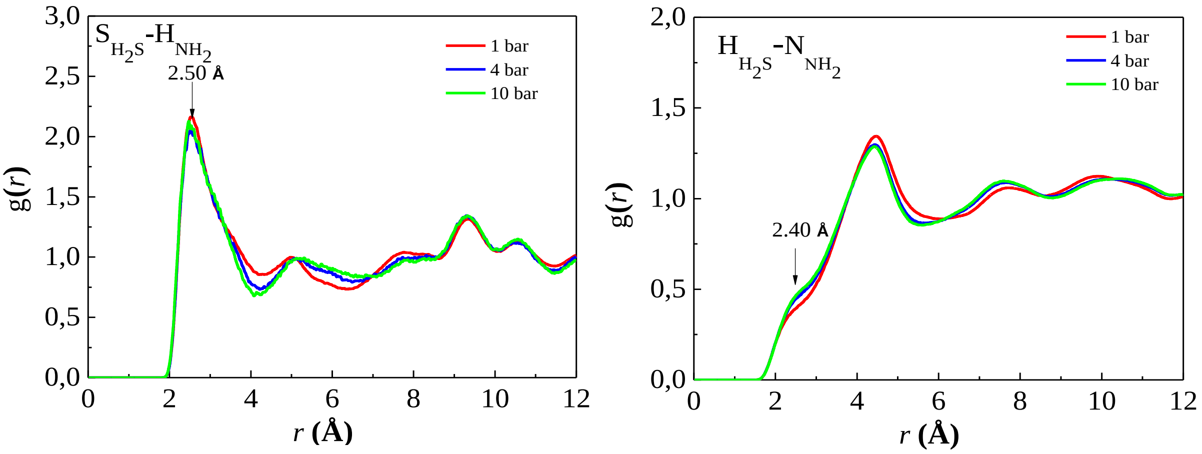

Figure S19. Radial distribution functions for the pairs S(H_2S)-H(NH_2) (left) and H(H_2S)-N(NH_2) (in MIL-125(Ti)-NH_2 at 303 K at 3 different pressures.

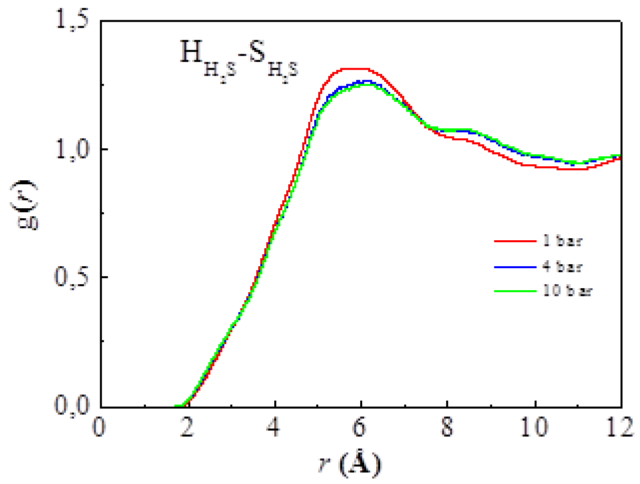

Figure S20. Radial distribution functions for the pair S(H_2S)-H(H_2S) in MIL-125(Ti)-NH_2 at 303 K at 3 different pressures.

4. Infrared spectra of CO_2 adsorbed on MIL-125(Ti) and MIL-125(Ti)-NH_2

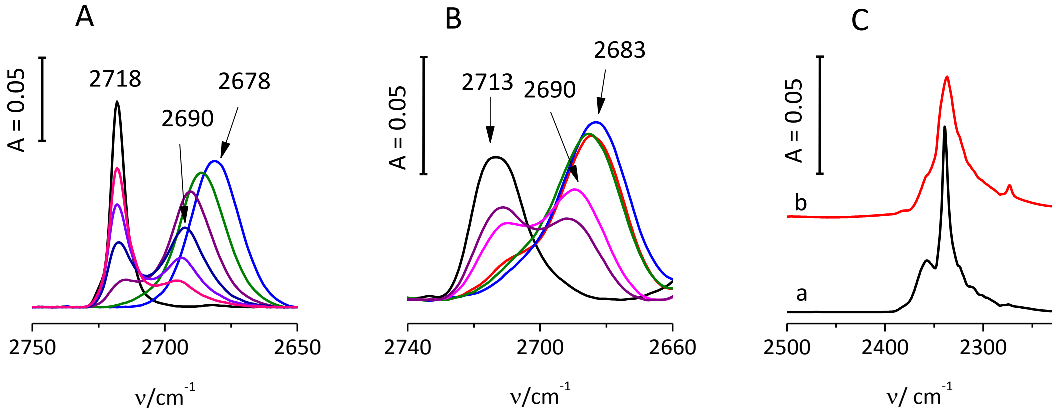

Figure S21. ν(OD) range of the spectra of MIL-125(Ti) (A) and MIL-125(Ti)-NH_2 (B) pretreated by D_2O and then activated at 170°C after adsorption of increasing doses of CO_2: (C) : spectra of MIL-125(Ti) (a) and MIL-125(Ti)-NH_2 (b) in the $\nu_3(CO_2)$ range. (CO_2 introduced at RT into the cell, 30 Torr excess over the sample, then cooled down to -60 °C).

Adsorbed CO_2 gives rise to two (ν1+ν3) combination bands at about 3700 and 3600 cm^{-1}, frequency range that overlaps that of the ν(OH) bands of the μ_2-OH group, preventing a clear interpretation of the IR spectrum in this domain. To circumvent this issue, before any CO_2 adsorption experiments on MIL-125(Ti) and MIL-125(Ti)-NH_2, the deuteration of hydroxyls groups has been performed with D_2O since the isotopic exchange shift the stretching hydroxyls band from 3686 cm^{-1} (ν(OH) vibration) to 2718 cm^{-1} (ν(OD) vibration), a range free of any band characteristic of the adsorbed CO_2. As observed in the case of H_2S adsorption, the CO_2 molecules interact at low temperature with the hydroxyls group of MIL-

125(Ti) leading to a shift of the ν(OD) band at full coverage from 2718 to 2678 cm^{-1} (see Figure SI21). This shift (Δν(OD) = 40 cm^{-1}) is the signature of linearly adsorbed CO_2 species hydrogen bonded to the hydroxyl groups via the O atom (μ_2-OD$\cdots$O=C=O).

5. Macroscopic model

The vacancy solution model originally proposed by Suwanayuen and Danner,[18-19] and adapted by Cochran *et al.*,[20-21] considers the adsorption equilibrium in terms of equilibrium between two vacancy solutions. So, both the gas phase and the adsorbed phase are composed of adsorbates and a hypothetical solvent: the vacancy. The vacancies represent voids in both solutions which can be replaced by adsorbates. Cochran *et al.* have shown the following general equations for adsorption isotherms and mixture adsorption equilibrium:

$$p = \frac{n_1^{s,\infty}\theta}{b_1(1-\theta)} \exp\left(-\int \frac{d\ln\gamma_3^s}{\theta}\right) \lim_{\theta\to 0}\left(\exp\left(\int \frac{d\ln\gamma_3^s}{\theta}\right)\right) \tag{S1}$$

$$\phi_i y_i p = \gamma_i^s x_i \frac{n_m^s n_i^{s,\infty}}{n_m^{s,\infty} b_i} \lim_{x_i^s\to 0}\left(\frac{1}{\gamma_i^s}\right) \exp\left(\frac{\pi\ a_i}{RT}\right) \tag{S2}$$

$$\frac{\pi\ a_i}{RT} = -\left[1+\left(\frac{n_m^{s,\infty}-n_i^{s,\infty}}{n_m^s}\right)\right]\ln\gamma_3^s x_3^s \tag{S3}$$

In equations (S1) to (S3), the subscript 3 represents the vacancy, $n_i^{s,\infty}$ is the number of adsorbed molecules at saturation, b_i is the Henry's law constant, θ is the fractional surface coverage. y_i and x_i are respectively the gas phase and the adsorbed phase mole fractions for component *i*. $n_m^{s,\infty}$ is the limiting amount adsorbed of gas mixture which is calculated as follow:

$$n_m^{s,\infty} = \sum_i x_i n_i^{s,\infty} \tag{S4}$$

n_m^s is the total moles adsorbed of mixture and x_i^s represents the mole fraction of component *i* in the adsorbed vacancy solution. It is defined as follow in terms of x_i :

$$x_i^s = \frac{x_i \; n_m^s}{n_m^{s,\infty}} = x_i \; \theta \text{ for i = 1 or 2} \tag{S5}$$

$$x_3^s = 1 - \theta \tag{S6}$$

π is the spreading pressure and a_i is the partial molar area. ϕ_i is the fugacity coefficient of component i in the gas phase. Finally, γ_i^s represents the activity coefficient of component *i* in the adsorbed phase. These coefficients can be defined by different thermodynamic theories. Suwanayuen and Danner used the Wilson expression whereas Cochran *et al.* used the Flory-Huggins equation. Others expressions can also be used like Margules equation,[18] or NRTL.[22] In this work, we used both the Wilson equations.

In the Wilson form, the expression of the activity coefficient is:

$$\ln \gamma_k^s = 1 - \ln\left[\sum_{j=1}^{j=N} x_j^s \Lambda_{kj}\right] - \sum_{i=1}^{i=N}\left[\frac{x_i^s \Lambda_{ik}}{\sum_{j=1}^{j=N} x_j^s \Lambda_{ij}}\right] \tag{S7}$$

The pure component adsorption isotherm and the equilibrium mixture adsorption equation are:

$$p = \frac{n_1^{s,\infty}}{b_1} \frac{\theta}{1-\theta}\left[\Lambda_{13} \frac{1-(1-\Lambda_{31})\;\theta}{\Lambda_{13}+(1-\Lambda_{31})\;\theta}\right] \exp\left(\frac{-\Lambda_{31}(1-\Lambda_{31})\;\theta}{1-(1-\Lambda_{31})\;\theta} - \frac{(1-\Lambda_{13})\;\theta}{\Lambda_{13}+(1-\Lambda_{13})\;\theta}\right) \tag{S8}$$

$$\phi_i y_i p = \gamma_i^s x_i \, n_m^s \frac{n_i^{s,\infty} \Lambda_{i3}}{n_m^{s,\infty} b_i} \exp(\Lambda_{3i} - 1) \exp\left(\frac{\pi \; a_i}{RT}\right) \tag{S9}$$

Λ_{i3} and Λ_{3i} represent interactions between the adsorbent and the adsorbate molecules. So each single component isotherm is defined by four parameters: $n_i^{s,\infty}, b_i$, Λ_{i3} and Λ_{3i}. It can be noticed that the adsorbate-adsorbate interactions (Λ_{ij}) are neglected compared with adsorbate-adsorbent interactions.

6. Mixture adsorption

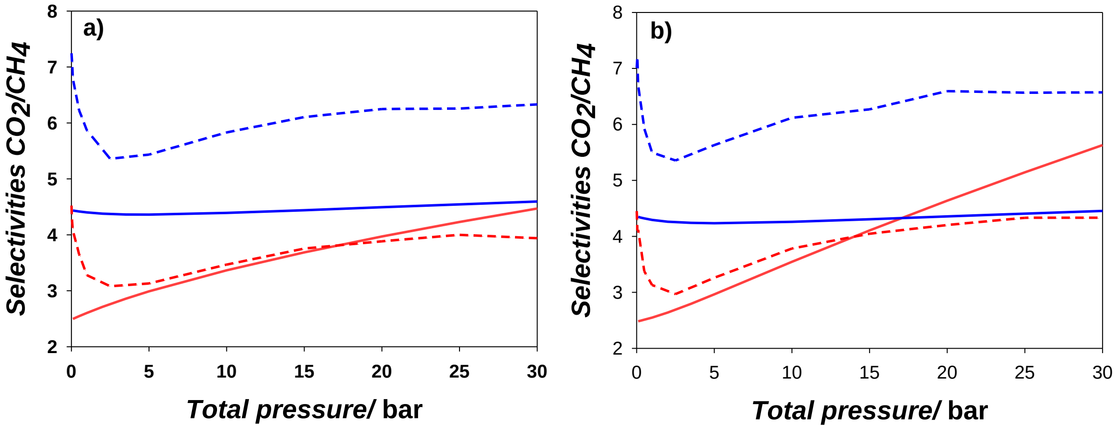

Figure S22. CO_2/CH_4 selectivities prediction, on MIL-125(Ti) (red) and MIL-125(Ti)-NH_2 (blue), by VSM theory (full lines) and GCMC simulations (dotted lines); molar ration in gaseous phase : 50-50% (a) and 75-25% (b)

Table S7: CO_2/CH_4 GCMC and VSM simulated selectivities at 303 K and 50/50 molar ratio.

GCMC prediction			VSM predictions		
p (bar)	**MIL-125(Ti)**	**MIL-125(Ti)-NH_2**	**p (bar)**	**MIL-125(Ti)**	**MIL-125(Ti)-NH_2**
0.1	4.0767	6.7863	0.1	2.4966	4.4344
0.5	3.6529	6.2282	0.5	2.5458	4.4167
1	3.2798	5.8692	1	2.6044	4.3998
5	3.1306	5.4331	5	2.9897	4.3618
10	3.4666	5.8301	10	3.3660	4.3916
15	3.7540	6.1049	15	3.6857	4.4403
20	3.8842	6.2486	20	3.9701	4.4929
25	3.9995	6.2567	25	4.2295	4.5452
30	3.9390	6.3307	30	4.4699	4.5959

Table S8: CO_2/CH_4 GCMC and VSM simulated selectivities at 303 K and 75/25 molar ratio.

GCMC prediction			VSM predictions		
p (bar)	**MIL-125(Ti)**	**MIL-125(Ti)-NH_2**	**p (bar)**	**MIL-125(Ti)**	**MIL-125(Ti)-NH_2**
0.1	4.1181	6.6999	0.1	2.4840	4.3482
0.5	3.3748	5.9188	0.5	2.5117	4.3202
1	3.1297	5.4963	1	2.5503	4.2945
5	3.2599	5.6301	5	2.9650	4.2349
10	3.7818	6.1180	10	3.5453	4.2600
15	4.0460	6.2686	15	4.1052	4.3061
20	4.2020	6.5928	20	4.6373	4.3563
25	4.3310	6.5642	25	5.1444	4.4062
30	4.3334	6.5720	30	5.6297	4.4546

Table S9: H_2S/CH_4 GCMC and VSM simulated selectivities at 303 K and 10 bar.

GCMC prediction			**VSM predictions**		
y H_2S	**MIL-125(Ti)**	**MIL-125(Ti)-NH_2**	**y H_2S**	**MIL-125(Ti)**	**MIL-125(Ti)-NH_2**
0.001	39.809	66.755	0.001	15.1064	35.3523
0.005	22.953	43.003	0.005	15.0996	35.0381
0.01	18.051	37.74	0.01	15.0886	34.8243
0.05	13.651	34.23	0.05	15.1347	35.0753
0.1	16.095	36.887	0.1	15.7623	36.2034

References

[1] M. Dan-Hardi, C. Serre, T. Frot, L. Rozes, G. Maurin, C. Sanchez, G. Férey, *J. Am. Chem. Soc*. **2009**, *131*, 10857.

[2] Dmol^3, Materials Studio, V5.5, Accelrys, Inc: San Diego, **2010.**

[3] A. K. Rappé, C. J. Casewit, K. S. Colwell, W. A. Goddard III and W. M. Skiff, *J. Am. Chem. Soc*. **1992**, *114*, 10024.

[4] A. L. Myers, P. A. Monson, *Langmuir* **2002**, *18*, 10261.

[5] O. Talu, A. L. Myers, *AIChE J.* **2001**, *47*, 1160.

[6] T. Düren, F. Millange, G. Férey, K. S. Walton and R. Q. Snurr, *J. Phys. Chem. C* **2007**, *111*, 15350.

[7] L. D. Gelb, K. E. Gubbins, *Langmuir* **1999**, *15*, 305.

[8] N. A. Ramsahye, G. Maurin, S. Bourrelly, P. L. Llewellyn, C. Serre, T. Loise, G. Férey, *J. Phys. Chem. C* **2008**, *112*, 514.

[9] Q. Yang, H. Jobic, F. Salles, D. Kolokolov, V. Guillerm, C. Serre, G. Maurin, *Chem.-Eur. J*. **2011**, *17*, 8882.

[10] M. G. Martin, J. I. Siepmann, *J. Phys. Chem. B* 1998, *102*, 2569.

[11] J. G. Harris, K. Hung, *J. Phys. Chem.* **1995**, *99*, 12021.

[12] G. Kamath, N. Lubna, J. J. Potoff, *J. Chem. Phys.* **2005**, *123*, 124505.

[13] W. L. Jorgensen, D. S. Maxwell, J. Tirado-Rives, *J. Am. Chem. Soc.* **1996**, *118*, 11225.

[14] C. D. Wick, J. M. Stubbs, N. Rai, J. I. Siepmann, *J. Phys. Chem. B* **2005**, *109*, 18974.

[15] Q. Yang, C. Zhong, *J. Phys. Chem. B* **2006**, *110*, 17776.

[16] T. J. H. Vlugt, E. García-Pérez, D. Dubbeldam, S. Ban and S. Calero, *J. Chem. Theory Comput.*, **2008**, *4*, 1107.

[17] A.L. Myers, J.M. Prausnitz, *AIChE J.* **1965,** 11, 121-127.

[18] S. Suwanayuen, R.P. Danner, *AIChE J.* **1980**, 26, 68-75.

[19] S. Suwanayuen, R.P. Danner, *AIChE J.* **1980**, 26, 76-83.

[20] T.W. Cochran, R.L. Kabel, R.P. Danner, *AIChE J.* **1985**, 31, 268-277.

[21] T.W. Cochran, R.L. Kabel, R.P. Danner, *AIChE J.* **1985**, 31, 2075-2082.

[22] K. Munakata, *J. Chem. Eng. Jpn.* **2007**, 40, 398-409.